Electronic Supplementary Material (ESI) for Nanoscale.

Capabilities of Transition Metals in Retarding the Bonding of Carbon Atoms to Minimize Dendritic Graphene

Zhenwei Zhu[a], Linjie Zhan[a], Wen Wan[a], Zhijuan, Zhao[a], Tien-Mo Shih[a,b], Weiwei Cai[a]*

[a]Department of Physics, State Key Laboratory of Physical Chemistry of Solid Surfaces, Xiamen University, 361005, China

[b]Institute for Complex Adaptive Matter, University of California, Davis, CA 95616, USA

*Email: wwcai@xmu.edu.cn.

Keywords: graphene, hexagonal, single layer, single crystal, high quality, transition metals

Supplementary information

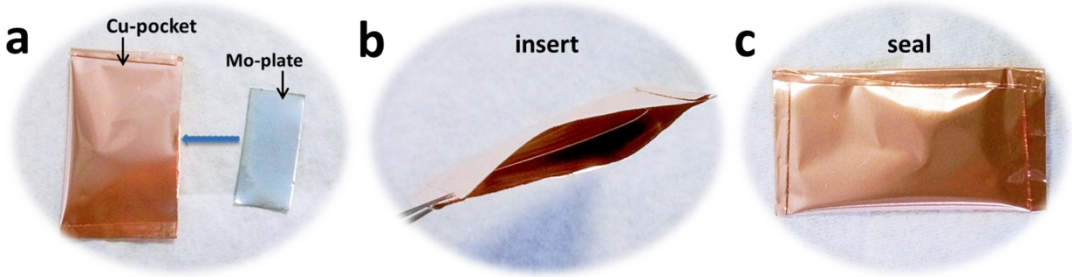

Figure S1. These photographs show the Cu pocket with a piece of Mo-plate manufacturing process. (a) A piece of prepared copper folds into a Cu-pocket. (b) Fit the size of Mo-plate into the Cu-pocket. (c) Seal the Cu-pocket.

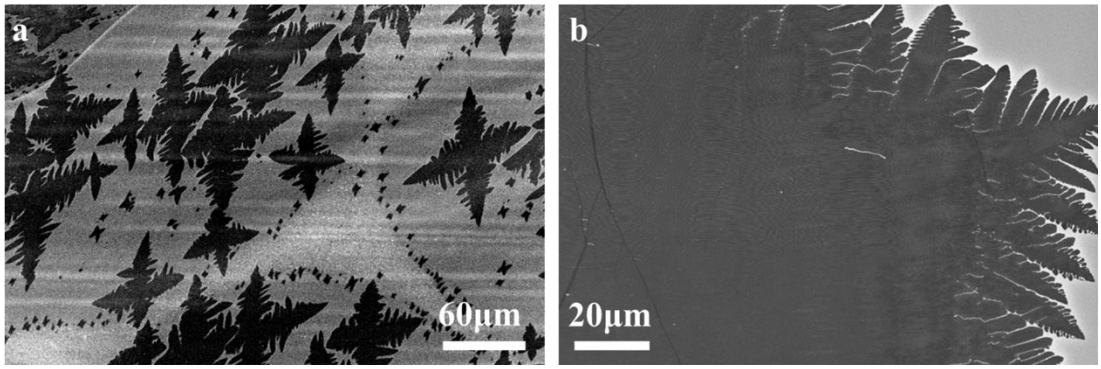

Figure S2. SEM images show that the graphene domains with rough edges.

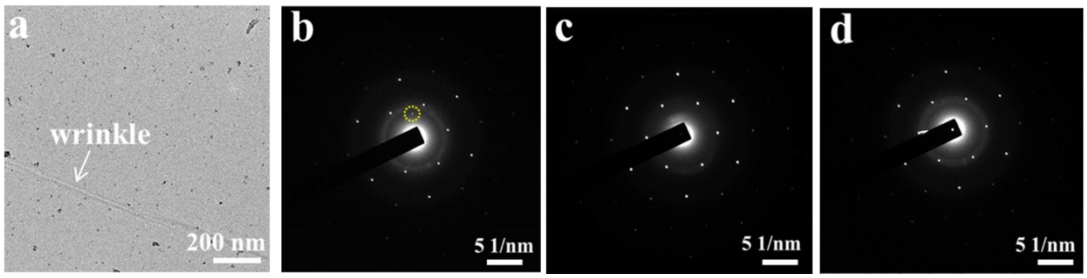

Figure S3. TEM image and SAED pattern (b-c) at three different locations on a hexagonal graphene domain.

Figure S3a shows the TEM image of an area of a hexagonal graphene domain. The SAED pattern in Figure S3b shows one independent spot (Yellow circle), which suggests the nature of 1D in the wrinkle. A slight distortion of the spots indicates a slight misorientation of graphene layers near the wrinkle.[1]

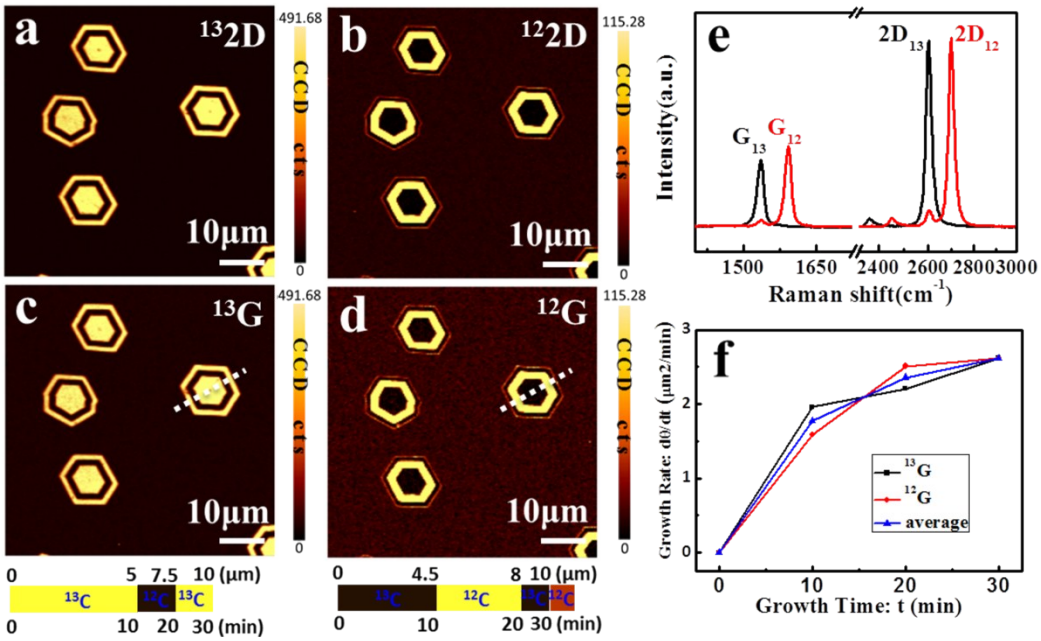

Figure S4. Raman spectra and mapping and growth rate of graphene domains.

The growth rate ($d\theta/dt$, coverage area θ) of graphene domains on Cu can be obtained from Raman mapping by carbon isotope-labeled growth. As shown in Figures S4a-d, the Raman 2D and G peak intensity maps of hexagonal graphene films directly depict the growth process. The growth conditions: a CH_4 flow of 1.5 sccm, a H_2 flow of 100 sccm, T=1080℃, and growth time for 30 min. Therefore, the growth rate can be extracted from the maps and plotted as a function of growth time (Fig. S4f). The $d\theta/dt$ of domains appears non-linear, and acceleration of growth rate becomes small. Finally, the size of graphene domains keeps approximate 20 μm.

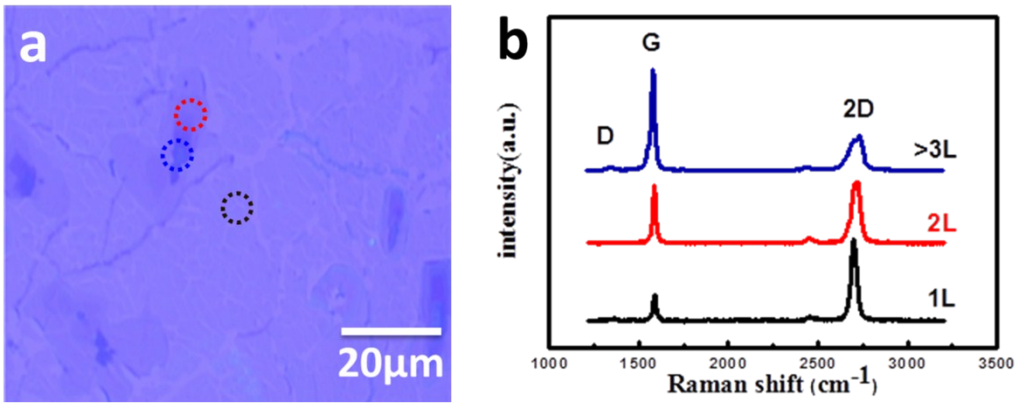

Figure S5. Multilayer graphene grown on Mo plate and transferred to 280 nm SiO_2/Si substrates. (a) An optical image of the multilayer graphene transferred to SiO_2/Si substrates by the bubbling transfer process. (b) Raman spectra of the mono-, bi- and multi-layer graphene take on the area marked with corresponding black, red, and blue dash circle in (a).

Figure S5a shows an optical micrograph of a graphene film grown on the Mo plate and transferred onto a 280 nm SiO_2/Si wafer by the bubbling method (Delighted in the Method). The graphene film can be clearly visualized due to its light interference. The variation of color contrast indicates the film is not uniform in thickness. Figure S5b shows Raman spectra taken from different layers in Fig. S5a. The intensity of the G band becomes more obvious, while the intensity of the 2D band broadens in an unobvious way and blue shifts.[2] These outcomes indeed indicate the status of AB-stacked (Bernal-stacked) in both bilayer graphene and multilayer graphene. Raman results reveal that graphene grown on Mo plate is governed by the dissolution and segregation mechanism, which is consistent with previous work.[3] According to metal-

C phase diagrams[4] and prior work[5, 6], we know that carbon species can react with Mo atoms and form into Mo carbides at the growth temperature.

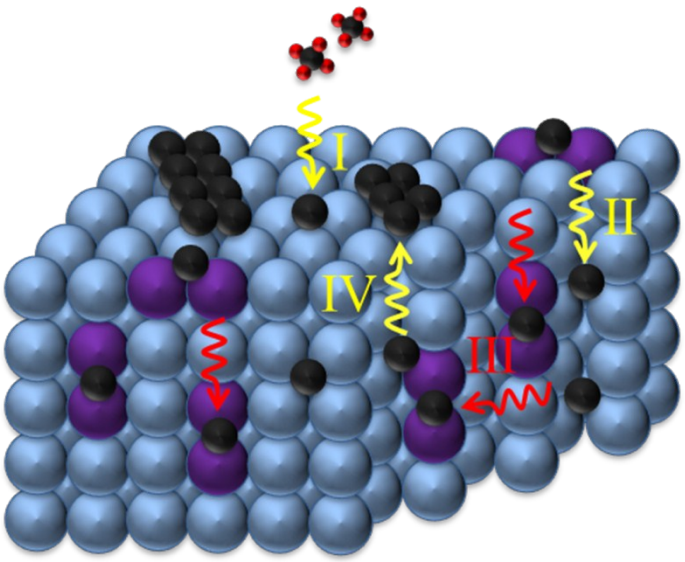

Figure S6. Schematic flowchart of the grow process with a Mo plate.

Figure S6 shows a schematic drawing of the Mo plate that controls graphene growth rate by suppressing the quantity of carbon source. The numbers from Ⅰ to Ⅳ represent the elementary steps of the Mo plate in the Cu pocket: (Ⅰ) surface catalytic decomposition of the carbon source and reconstruction of the carbons, (Ⅱ) some of them dissolve into the Mo sub-surface and bulk, (Ⅲ) the formation of Mo carbides and suppress upward precipitation of the carbons, and (Ⅳ) some of the dissolved carbon atoms precipitate from Mo bulk to surface during the cooling stage. The reduction of active carbon atoms in Cu pocket suppresses the growth rate of graphene on interior surface of Cu pocket.

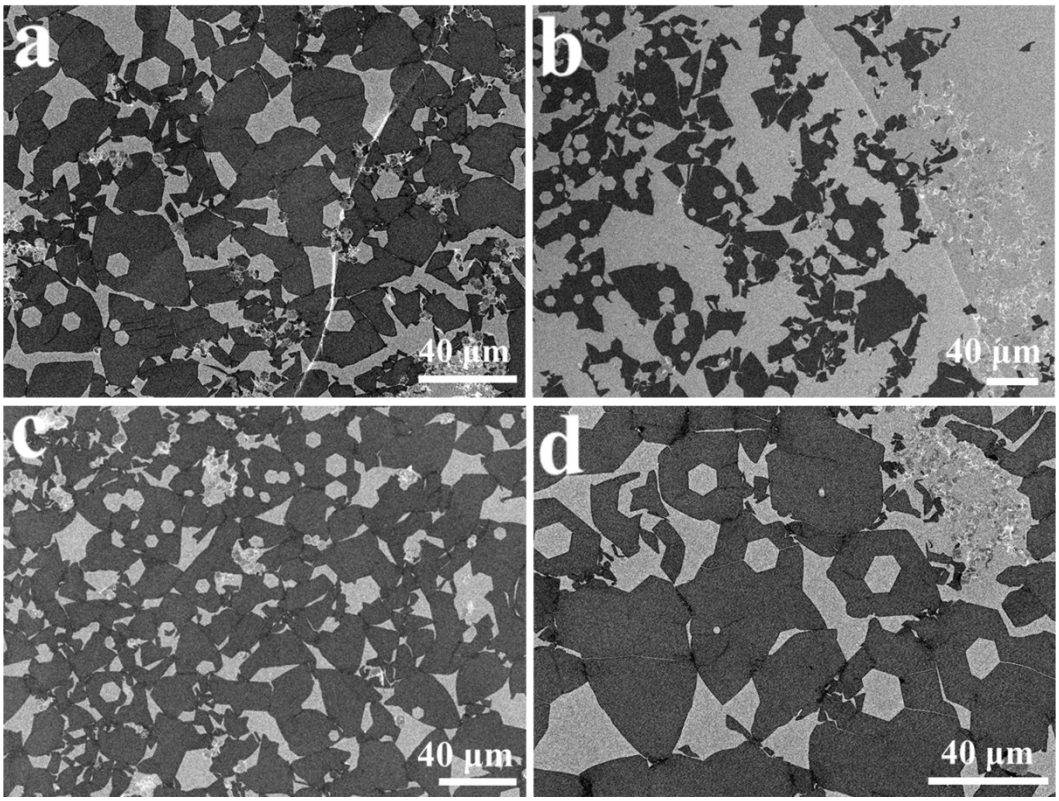

Figure S7. SEM images of graphene flake with hexagonal region etched.

We found graphene flakes with very regular hexagonal openings on the exterior surface of a Cu pocket while we got the ultrathin Mo_2C crystal. We believe that the Mo atoms diffused from the interior surface break the C-C bond of graphene in where etching reaction is initiated.

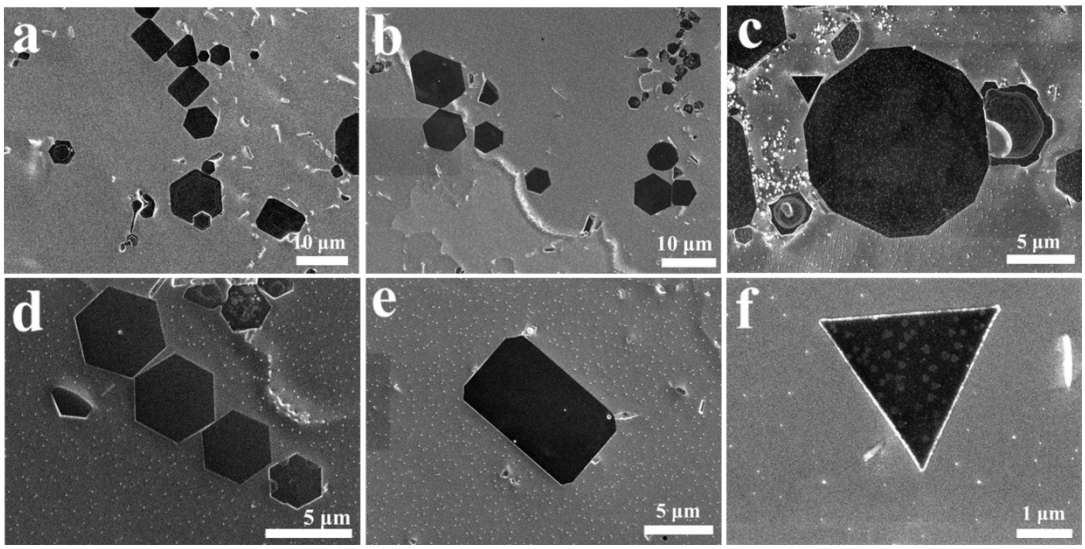

Figure S8. SEM images of ultrathin Mo_2C crystals on the Cu substrate, showing different shape (a, b). (c) Triangle and dodecagon, (d) hexagon, (e) octagon, (f) triangle.

We can also fabricate ultrathin Mo_2C crystals at high temperature of 1090℃ on the exterior surface of a Cu pocket that is inserted a Mo plate, while the other experimental parameters remained the same as Fig. S4.

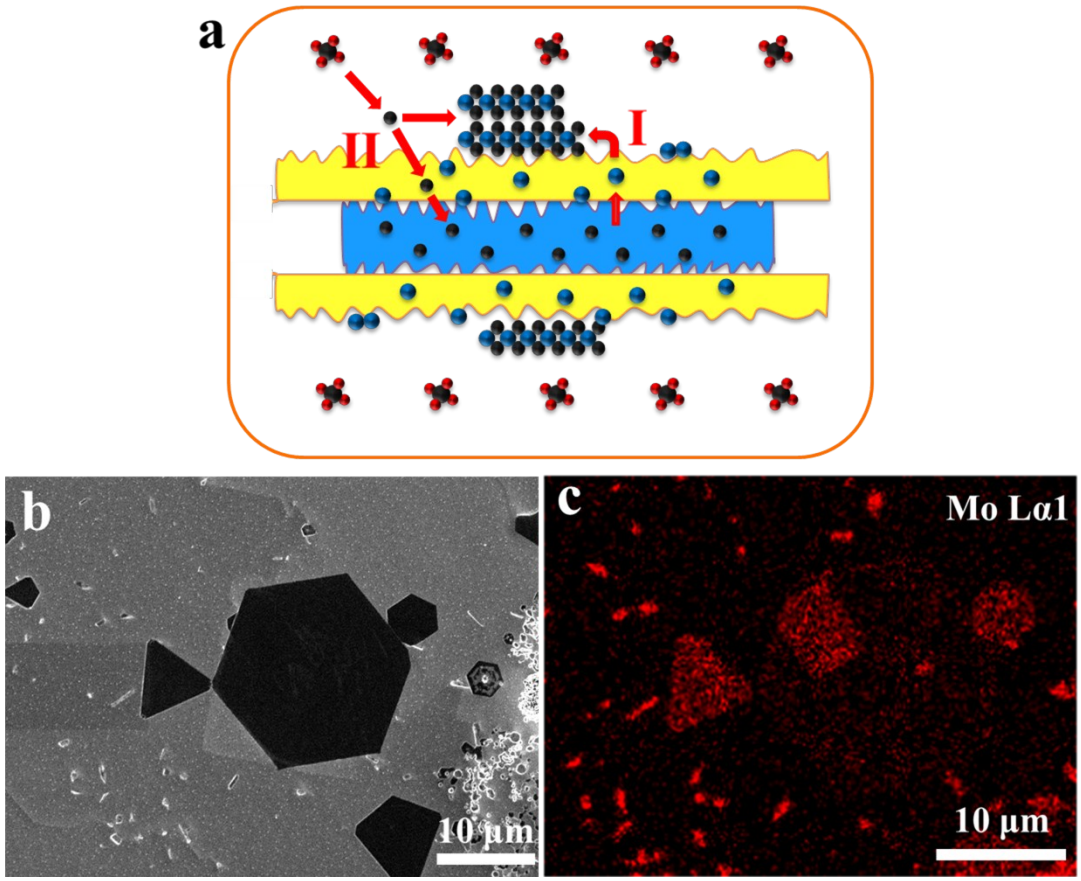

Figure S9. Schematic diagram and characterization of synthesizing ultrathin Mo_2C crystals on the Cu substrate.

The high growth temperature allows the Cu to melt and a Mo-Cu alloy is formed at the liquid Cu/Mo interface.[7] Subsequently, (Ⅰ) Mo atoms diffuse from the interior surface to the exterior surface of the Cu pocket, (Ⅱ) diffused out Mo atoms react with the carbon atoms which come from the decomposition of methane. Figure S9b depicts SEM image of a rectangular crystal filled together with a hexagonal domain. We are capable of scanning more clearly by the EDS elemental mapping (Fig. S9c).

Supplementary References

1. S. J. Chae, F. Güneş, K. K. Kim, E. S. Kim, G. H. Han, S. M. Kim, H.-J. Shin, S.-M. Yoon, J.-Y. Choi, M. H. Park, C. W. Yang, D. Pribat and Y. H. Lee, *Adv. Mater.*, 2009, **21**, 2328-2333.
2. A. C. Ferrari, J. C. Meyer, V. Scardaci, C. Casiraghi, M. Lazzeri, F. Mauri, S. Piscanec, D. Jiang, K. S. Novoselov, S. Roth and A. K. Geim, *Phys. Rev. Lett.*, 2006, **97**, 187401.
3. B. Wang, Y. Zhang, Z. Chen, Y. Wu, Z. Jin, X. Liu, L. Hu and G. Yu, *Mater. Lett.*, 2013, **93**, 165-168.
4. Y. Wu, G. Yu, H. Wang, B. Wang, Z. Chen, Y. Zhang, B. Wang, X. Shi, X. Xie, Z. Jin and X. Liu, *Carbon*, 2012, **50**, 5226-5231.
5. B.-J. Lee and G.-H. Jeong, *Appl. Phys. A*, 2014, **116**, 15-24.
6. B. Dai, L. Fu, Z. Zou, M. Wang, H. Xu, S. Wang and Z. Liu, *Nat. Commun.*, 2011, **2**, 522.
7. C. Xu, L. Wang, Z. Liu, L. Chen, J. Guo, N. Kang, X. L. Ma, H. M. Cheng and W. Ren, *Nat. Mater.*, 2015, **14**, 1135-1141.